

Model calculations of the static distribution of the electric-field-gradient tensor elements in substitutionally disordered $\text{Rb}_{1-x}(\text{NH}_4)_x\text{H}_2\text{PO}_4$

R. Kind

Laboratorium für Festkörperphysik, Eidgenössische Technische Hochschule Zürich–Hönggerberg, CH-8093 Zürich, Switzerland

R. Blinc and M. Koren

J. Stefan Institute, E. Kardelj University of Ljubljana, YU-61111 Ljubljana, Yugoslavia

(Received 6 July 1987)

The substitution of Rb by NH_4 in RbH_2PO_4 results in competing interactions of the ferroelectric-antiferroelectric type, which for a certain concentration range $0.22 < x < 0.78$ inhibit the onset of long-range proton order. In this system the local random polarization of the protons $p(x,t)$ couples linearly to the random-field variable $h(x,t)$. There is, however, always a static temperature-independent component $h_0(x)$ present which is due to the static random distribution of NH_4 and Rb. Quadrupole-perturbed NMR is a very suitable tool to measure the random-field distribution since the random polarization is mapped into the NMR line shape. The temperature dependence of the line shape allows for a clear separation between the static and dynamic components. In order to elucidate the influence of the static random field on the line shape we have performed model calculations of the five irreducible electric-field-gradient tensor-element distributions as a function of concentration. We demonstrate that these distributions are uncorrelated Gaussian distributions.

I. INTRODUCTION

The static or quasistatic distribution of the local random spin or pseudospin magnetization plays an important role in the theory of spin-glass transitions.¹⁻³ These systems are, however, not suitable for nuclear magnetic resonance (NMR) investigations, because of the strong coupling of the external magnetic field B_0 to the magnetic moments.⁴ In a proton glass [e.g., $\text{Rb}_{1-x}(\text{NH}_4)_x\text{H}_2\text{PO}_4$], this complication does not occur, but due to the random substitutional disorder a static random field is introduced. This static random field acts in the same way on the system as a weak magnetic field acts on a diluted ferromagnet,⁵ i.e., the proton glass ordering sets in well above the T_c of the zero field phase transition. In order to measure the glass order parameter and the distribution of the local random field—which is proportional to the local random polarization p —by means of quadrupole perturbed NMR, we first have to take care of the influence of the NH_4 -Rb random distribution on the NMR line shape.

In Ref. 6 we assumed that the NH_4 -Rb distribution leads to independent Gaussian distributions of the five irreducible tensor elements of the electrical-field-gradient (EFG) tensor at the Rb site, and we have used this assumption to calculate the orientational dependence of the ^{87}Rb ($-\frac{1}{2}-+\frac{1}{2}$) line shape. By comparing the measured orientational dependence of the line shape with the theoretical one, we were able to separate the contributions of the different EFG tensor elements.

In this contribution we demonstrate by means of model calculations that our basic assumptions were correct. The distribution of the EFG tensor elements is indeed

Gaussian, and all linear correlation coefficients between these distributions are zero within the limits of the statistical error.

II. STATIC DISPLACEMENT MODELS FOR RADP

In order to calculate the distribution of the EFG tensor elements we use a simple point-charge model. The contribution of a point charge $Q(r)$, where $r^2 = x_1^2 + x_2^2 + x_3^2$, to the EFG tensor at the origin is given by

$$V_{jk} = Q \left[\frac{3x_j x_k}{r^5} - \delta_{jk} \frac{1}{r^3} \right]. \quad (1)$$

The total EFG tensor is then given by the lattice sum over all charges within a certain range. The convergence of this sum is rather bad ($1/r$ dependence), and the result is often size and shape dependent. In our case, however, we are not interested in the absolute values of the EFG tensor elements, but only in the distribution of these elements around their mean values. We now assume that this distribution is the result of small displacements of point charges in the unit cell from the ideal unperturbed structure. The deviation from the contribution given by Eq. (1) is then given by

$$\Delta V_{jk} = \sum_{l=1}^3 V_{jkl} \Delta x_l, \quad (2)$$

where the Δx_l are the displacements of the point charge and V_{jkl} is given by

$$V_{jkl} = Q \left[-\frac{15x_j x_k x_l}{r^7} + \delta_{jl} \frac{3x_k}{r^5} + \delta_{kl} \frac{3x_j}{r^5} + \delta_{jk} \frac{3x_l}{r^5} \right]. \quad (3)$$

The lattice sum to obtain ΔV_{jk} for a given set of displacements converges now as $1/r^2$, which for our case means that more than 90% of the contribution comes from a range within ± 2 lattice constants.

We assume now that the substitution of a Rb atom by an ammonium group in pure RbH_2PO_4 (RADP) leads to a small lattice distortion around the NH_4 group which affects mainly the surrounding PO_4 groups. For the sake of simplicity we assume a point charge at the center of each PO_4 group. Furthermore, we neglect all other

$$\text{Rb(1)}:(0,0,0); \text{Rb(2)}:(\frac{1}{2}, 0, \frac{1}{4}); \text{Rb(3)}:(\frac{1}{2}, \frac{1}{2}, \frac{1}{2}); \text{Rb(4)}:(0, \frac{1}{2}, \frac{3}{4});$$

$$\text{P(1)}:(\frac{1}{2}, \frac{1}{2}, 0); \text{P(2)}:(0, \frac{1}{2}, \frac{1}{4}); \text{P(3)}:(0, 0, \frac{1}{2}); \text{P(4)}:(\frac{1}{2}, 0, \frac{3}{4}).$$

For the calculations 216 unit cells were taken into account (i.e., ± 3 lattice constants in each direction from the origin). For each site (except for the origin which is always occupied by a Rb atom), a random number generator had to decide with the probability x whether it is occupied by an ammonium or by a Rb atom with the probability $(1-x)$, respectively. In case of an NH_4 group, the adjacent PO_4 groups are displaced according to one of the models described later in this section. For the displaced PO_4 groups the contribution to the ΔV_{jk} was calculated and taken into account in the sum of Eq. (2). For one run through the lattice, one obtains one set of ΔV_{jk} . The distribution functions $P(\Delta V_{jk})$ are obtained by calculating histograms from multiple repetitions (10^4 times) of the whole procedure. The distributions were calculated for the five irreducible elements of the EFG tensor V_{zz} , V_{xz} , V_{yz} , V_{xy} , and $(V_{xx} - V_{yy})$. These are the only elements which enter into the nuclear quadrupole Hamiltonian. In order to save computer time the displacements were set to unity. This is justified by the linearity of Eq. (2), as well as by the fact that a point-charge model is not able to provide the proper absolute values of the standard deviations of the ΔV_{jk} anyhow.

A. The closest-neighbor model

Each NH_4 group in RADP has six nearest-neighbor PO_4 groups, but two of them are somewhat closer. These are the two PO_4 groups above and below the NH_4 in the z direction. The distance between the N and P atoms in the unperturbed lattice is $c/2$, where c is the lattice constant in the z direction. Due to the fact that the NH_4 group forms N-H—O bonds to the four lateral PO_4 groups, it is oriented in such a way⁷ that it needs slightly less space in the z direction than a Rb atom would take. Thus, if a PO_4 group is sandwiched in the z direction between a Rb atom and an NH_4 group, it is shifted towards the NH_4 group.

This very simple model turned out to be too discrete, especially for the calculation of $P(\Delta V_{zz})$. This distribution exhibited three well-separated maxima—with a separation of the order of the standard deviation—for an NH_4 concentration of $x = 0.5$ (Fig. 1). On lowering or

charges (or their displacements, respectively) in the system. This is, of course, a very rough approximation which by no means reflects the real charge distribution in RADP, but, nevertheless, one can obtain valuable information from this model.

Since we are interested in the Rb EFG tensor distribution, we have shifted the origin of the unit cell into the Rb(1) site. The new coordinates of the Rb and P atoms thus become

rising the concentration, these peaks became even more pronounced. Such behavior is not observed in the experiment, as the line shapes are reasonably good Gaussians and do not show any splittings for any concentration. The reason for the failure of the above model is that the contributions $V_{zz}\Delta z$ rapidly decay with increasing distance of the corresponding charges from the origin. The contributions V_{zz} of the two closest PO_4 groups have a relative weight of 12 603, the four next nearest-neighbor PO_4 groups have a relative weight of 2 881, the next eight a weight of 180, etc. The appearance of discrete peaks in the theoretical line shape thus results from the fact that the spectra are dominated by the contribution of the two closest PO_4 groups with four displacement possibilities only:

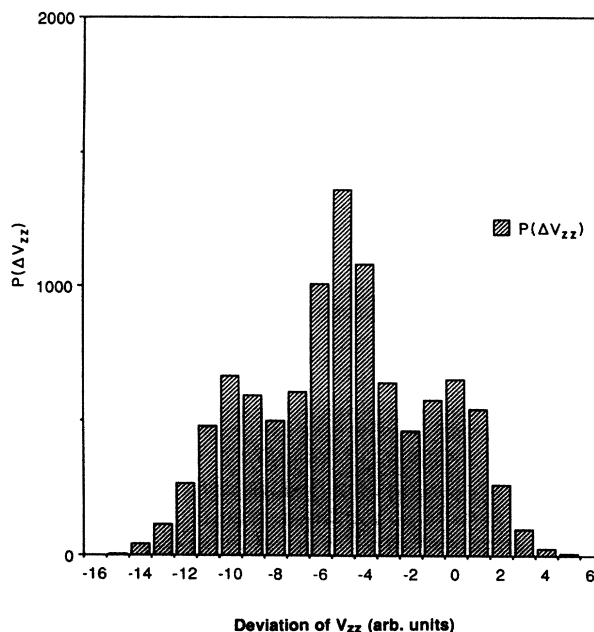


FIG. 1. Distribution P of ΔV_{zz} in the closest-neighbor model without elastic-distortion corrections for a total number of 10^4 samples for the NH_4 content, $x = 0.5$.

TABLE I. Relative standard deviations of the EFG tensor elements for the different displacement models compared with the measured values of D-RADP(44). The σ_{ij} stand for the $\sigma(\Delta V_{ij})$.

Model	σ_{xz}/σ_{zz}	σ_{xy}/σ_{zz}	$\sigma_{xx-yy}/\sigma_{zz}$
Closest neighbor	0.26	0.05	1.02
Bond	2.95	2.05	2.76
Combined equal signs	1.12	0.64	1.59
Combined different signs	0.49	0.41	1.59
D-RADP(44)	0.79		1.05

- (1) no displacements, $\Delta V_{zz} = 0$;
- (2) shift of upper PO_4 towards origin, $\Delta V_{zz} = -12\,603$;
- (3) shift of lower PO_4 towards origin, $\Delta V_{zz} = -12\,603$;
- (4) shift of both PO_4 towards origin, $\Delta V_{zz} = -25\,206$.

The displacements of all other PO_4 groups can broaden these three discrete peaks but cannot smear them out sufficiently. To overcome this problem we have to allow secondary or even tertiary displacements of the PO_4 groups, i.e., we have to increase the range of the lattice distortion induced by the NH_4 groups. This very important result clearly shows that the range of the relevant primary displacement contributions to the EFG tensor is smaller than the range of the lattice distortions, i.e., a single NH_4 group at some distance from the origin affects the EFG tensor at the origin much more by the distortion extended to the origin than the ΔV_{jk} of the local primary displacements. This effect is, of course, even more important for low NH_4 concentrations or—because of the symmetry of the problem—for NH_4 concentrations close to 1, respectively. One should therefore use an elastic distortion model for the displacements. A proper calculation of such a model would, however, consume too much computer time.

We therefore decided to use a simplified elastic distortion model. In this model we do not displace only the two closest PO_4 groups of a given NH_4 group in the z direction, but also the two sets of four PO_4 groups which are connected by O—H—O hydrogen bonds to the initially displaced ones. The amplitude of these secondary displacements is set to $\frac{1}{3}$ of the primary one. With this correction, nearly perfect Gaussian distributions were obtained for all tensor elements for an NH_4 concentration of $x=0.5$, and even for $x=0.1$ the distributions were fairly well Gaussian, i.e., nearly perfect in the tails, but with some significant deviations in the center of the distributions. From this one can see that for further improvement one would first have to improve the elastic distortion model.

Another defect of the closest-neighbor model is that the ratio of the calculated standard deviations $\sigma(\Delta V_{jk})$ of the EFG tensor components does not correspond to the measured ratios [e.g., for the deuterated compound with $x=0.44$, D-RADP(44)].⁸ The standard deviations of V_{xz} and V_{yz} are too small by a factor of 3 as compared to the measured ratio (see Table I).

An interesting result of the closest-neighbor model is a linear concentration-dependent negative shift in the average of ΔV_{zz} . Such a shift was indeed observed in the experiment although it does not depend linearly on the con-

centration. All other tensor elements are distributed around zero in this model, i.e., in reality around the values of the unperturbed lattice.

B. The bond model

As already mentioned in the preceding subsection, the NH_4 groups form N—H—O bonds to the four lateral PO_4 groups. We now assume that these four PO_4 groups are pulled in the direction of the corresponding bonds towards the NH_4 group. For the sake of simplicity the corresponding displacements are performed either only in the x direction or only in the y direction, whichever is closer to the bond direction. The displacement is, of course, cancelled if two NH_4 groups pull from opposite sides of the PO_4 group.

This model yields perfect Gaussian distributions of the ΔV_{jk} for the concentration $x=0.5$ without any further corrections. For $x=0.1$, however, significant deviations from Gaussian distributions in the center (sharpening of the center) indicate that this model also should be improved by an elastic distortion correction. Since the distributions were still nearly perfect Gaussian in the tails, one can expect that the standard deviations will not much change by such a correction, and therefore we abstained from an improvement of this model.

This model also did not yield the measured ratios between the standard deviations of the ΔV_{jk} , but here the situation is complementary to the one of the closest-neighbor model. The standard deviations of ΔV_{xz} and ΔV_{yz} are too large by a factor of 4 as compared to the measured ratio (see Table I). From this result it is obvious that we have to combine the two models in order to obtain the proper ratios of the $\sigma(V_{jk})$.

C. The combined model

Since the distributions of the corresponding EFG tensor elements of the two above-mentioned models are linearly correlated, the resulting distributions of the combination not only depend on the relative amplitudes but also on the relative signs of the displacements used in the two models. Concerning the signs, better results were obtained for equal signs than for opposite ones. This corresponds, e.g., to an all-attraction model, i.e., all six nearest-neighbor PO_4 groups are attracted by the NH_4 group. The corresponding distributions are shown in Figs. 2(a)–2(d), and the ratios of the standard deviations $\sigma(\Delta V_{jk})/\sigma(\Delta V_{zz})$ are given in Table I. For illustration,

the corresponding ratios are also given for the combined model with opposite signs. One could now try to also fit the relative amplitudes to have better agreement with the experiment, but because of the very rough approximations used in our models this would not be meaningful at all.

The concentration dependence of the standard deviations $\sigma(\Delta V_{jk})$ is shown in Fig. 3 for the combined model with equal signs and amplitudes. The solid lines correspond to a fit with the function

$$\sigma(\Delta V_{jk}) = c_{jk} [x(1-x)]^{1/2},$$

where the c_{jk} are the fit parameters. One can see that there is a symmetry with respect to the concentration $x=0.5$ and that the ratios of the $\sigma(\Delta V_{jk})$ do not depend on the concentration. For real systems of D-RADP this symmetry does not exist at room temperature. One reason for this might be that for some concentrations there is already an incipient glassy-type ordering at this temperature.

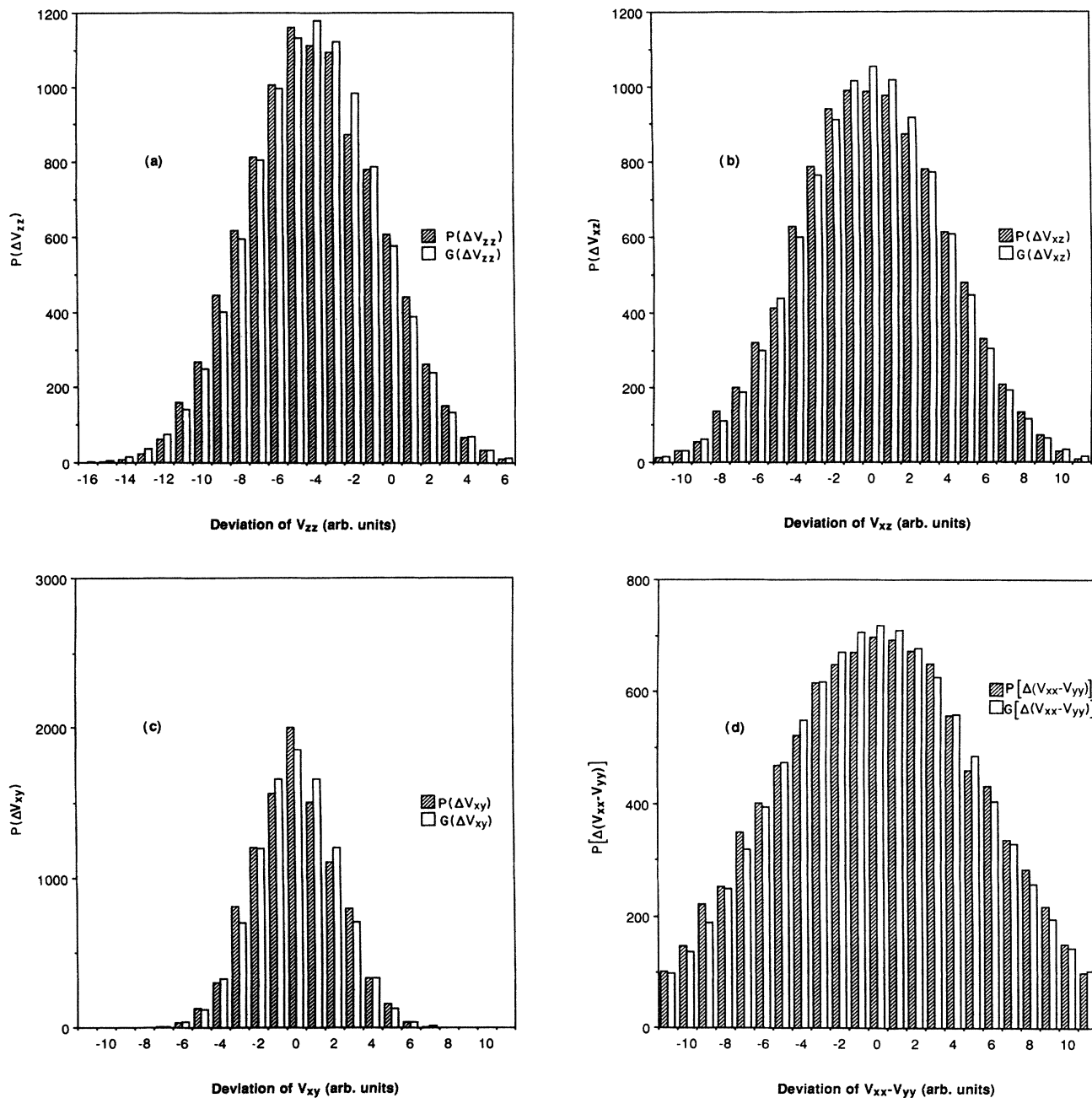


FIG. 2. Distribution P of ΔV_{zz} (a), ΔV_{xz} (b), ΔV_{xy} (c), and $\Delta(V_{xx}-V_{yy})$ (d) in the combined model for 10^4 samples for the NH_4 content $x=0.5$. The distributions G are calculated Gaussian distributions with the same means and variances.

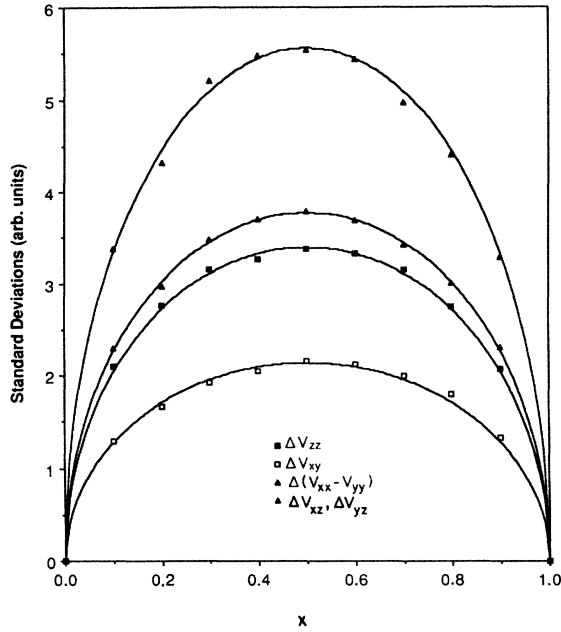


FIG. 3. Calculated standard deviations $\sigma(\Delta V_{jk})$ vs NH_4 content x in $\text{Rb}_{1-x}(\text{NH}_4)_x\text{H}_2\text{PO}_4$ for the combined model. The solid lines correspond to a fit with the function $\sigma(\Delta V_{jk}) = c_{jk}[x(1-x)]^{1/2}$. Due to the tetragonal symmetry of the model we have $\sigma(\Delta_{xz}) = \sigma(\Delta V_{yz})$.

III. STATISTICAL CONSIDERATIONS

One important point we wanted to check with our models is whether there is some correlation between the distributions of the ΔV_{jk} , because all of them contribute to the NMR line shape. The standard deviations of these contributions depend in different complicated ways on the orientation of the crystal in the external magnetic field B_0 . The total line shape of a given orientation is then determined by a convolution of the individual resulting frequency distributions. In the case of uncorrelated individual Gaussian distributions the resulting line shape is again Gaussian with a standard deviation given by

$$\sigma_{\text{tot}} = \left[\sum_i \sigma_i^2 \right]^{1/2}. \quad (4)$$

From the measured orientational dependence of σ_{tot} one can thus obtain the $\sigma(\Delta V_{jk})$ since their relation with the σ_i is known (for more details see Ref. 6). Equation (4) is valid, however, only for completely uncorrelated frequency distributions, i.e., for uncorrelated distributions of the ΔV_{jk} . We therefore have calculated the linear correlation coefficients r for all possible pairs of ΔV_{jk} distributions. This coefficient is given by

$$r = \frac{\sum_i (x_i - \bar{x})(y_i - \bar{y})}{\left[\sum_i (x_i - \bar{x})^2 \right]^{1/2} \left[\sum_i (y_i - \bar{y})^2 \right]^{1/2}}, \quad (5)$$

where x_i and y_i stand for the ΔV_{jk} , and \bar{x} is the mean of the x_i 's and \bar{y} is the mean of the y_i 's. The value of r lies between -1 and 1 , inclusive. A value of r near zero indicates that the variables x and y are uncorrelated. In the case of no correlation r is distributed approximately normally, with a mean of zero and a standard deviation of $1/(N)^{1/2}$, where N is the number of samples. In our models we have calculated 10^4 samples, i.e., the standard deviation $\sigma(r) = 0.01$. Most of the calculated r values were smaller than 0.01 , and very few reached values as high as 0.02 . That means that we can safely state that the ΔV_{jk} are uncorrelated in all our models. This result is not restricted to the substitutional disorder in RADP, but seems to be valid for similar systems with a random distribution of defects.

IV. CONCLUSIONS

We have shown by means of simple point-charge displacement models that a random substitutional disorder as present, e.g., in the mixed crystal system $\text{Rb}_{1-x}(\text{NH}_4)_x\text{H}_2\text{PO}_4$ yields uncorrelated Gaussian distributions of the five irreducible EFG tensor elements around their mean values. This is a very important starting point for further calculations where glassy-type proton ordering will be taken into account. With the help of these calculations and measured ^{87}Rb NMR line shapes, one can determine the random-field distribution and the glass order parameters as a function of temperature.

ACKNOWLEDGMENT

This work was supported in part by the Swiss National Science Foundation.

¹S. F. Edwards and P. W. Anderson, J. Phys. F 5, 968 (1975).

²G. Parisi, Phys. Rev. Lett. 43, 1954 (1973); 50, 1946 (1983).

³J. A. Hertz, Phys. Rev. Lett. 51, 1880 (1983).

⁴M. C. Chen and C. P. Slichter, Phys. Rev. B 27, 278 (1983).

⁵R. Pirc, B. Tadic, and R. Blinc, Phys. Rev. B 36, 8607 (1987).

⁶R. Kind, O. Liechti, R. Brüscheiler, J. Dolinsek, and R. Blinc, Phys. Rev. B 36, 13 (1987).

⁷A. W. Hewat, Nature 246, 90 (1973).

⁸R. Kind and M. Mohr (unpublished).